Translation Optics for 30 cm Ion Engine Thrust Vector Control

Thomas Haag
Glenn Research Center, Cleveland, Ohio

The NASA STI Program Office . . . in Profile

Since its founding, NASA has been dedicated to the advancement of aeronautics and space science. The NASA Scientific and Technical Information (STI) Program Office plays a key part in helping NASA maintain this important role.

The NASA STI Program Office is operated by Langley Research Center, the Lead Center for NASA's scientific and technical information. The NASA STI Program Office provides access to the NASA STI Database, the largest collection of aeronautical and space science STI in the world. The Program Office is also NASA's institutional mechanism for disseminating the results of its research and development activities. These results are published by NASA in the NASA STI Report Series, which includes the following report types:

- TECHNICAL PUBLICATION. Reports of completed research or a major significant phase of research that present the results of NASA programs and include extensive data or theoretical analysis. Includes compilations of significant scientific and technical data and information deemed to be of continuing reference value. NASA's counterpart of peer-reviewed formal professional papers but has less stringent limitations on manuscript length and extent of graphic presentations.

- TECHNICAL MEMORANDUM. Scientific and technical findings that are preliminary or of specialized interest, e.g., quick release reports, working papers, and bibliographies that contain minimal annotation. Does not contain extensive analysis.

- CONTRACTOR REPORT. Scientific and technical findings by NASA-sponsored contractors and grantees.

- CONFERENCE PUBLICATION. Collected papers from scientific and technical conferences, symposia, seminars, or other meetings sponsored or cosponsored by NASA.

- SPECIAL PUBLICATION. Scientific, technical, or historical information from NASA programs, projects, and missions, often concerned with subjects having substantial public interest.

- TECHNICAL TRANSLATION. English-language translations of foreign scientific and technical material pertinent to NASA's mission.

Specialized services that complement the STI Program Office's diverse offerings include creating custom thesauri, building customized data bases, organizing and publishing research results . . . even providing videos.

For more information about the NASA STI Program Office, see the following:

- Access the NASA STI Program Home Page at *http://www.sti.nasa.gov*

- E-mail your question via the Internet to help@sti.nasa.gov

- Fax your question to the NASA Access Help Desk at 301–621–0134

- Telephone the NASA Access Help Desk at 301–621–0390

- Write to:
  NASA Access Help Desk
  NASA Center for AeroSpace Information
  7121 Standard Drive
  Hanover, MD 21076

Translation Optics for 30 cm Ion Engine Thrust Vector Control

Thomas Haag
Glenn Research Center, Cleveland, Ohio

National Aeronautics and
Space Administration

Glenn Research Center

Available from

Translation Optics for 30 cm Ion Engine Thrust Vector Control

Thomas W. Haag
National Aeronautics and Space Administration
Glenn Research Center
Cleveland, Ohio 44135

Data were obtained from a 30 cm xenon ion thruster in which the accelerator grid was translated in the radial plane. The thruster was operated at three different throttle power levels, and the accelerator grid was incrementally translated in the X, Y, and azimuthal directions. Plume data was obtained downstream from the thruster using a Faraday probe mounted to a positioning system. Successive probe sweeps revealed variations in the plume direction. Thruster perveance, electron backstreaming limit, accelerator current, and plume deflection angle were taken at each power level, and for each accelerator grid position. Results showed that the thruster plume could easily be deflected up to 6 degrees without a prohibitive increase in accelerator impingement current. Results were similar in both X and Y direction.

Introduction

The relative radial alignment between the screen and accelerator apertures of an ion thruster influences the path of exiting charged particles. Positively charged xenon ions are attracted to the negatively charged accelerator grid, which extracts ions from the thruster. If alignment between the screen and accelerator apertures is perfectly concentric, the radial influence on the ion path is cancelled due to symmetry and particles leave the thruster approximately along the aperture axis. If the accelerator aperture is radially offset from the axis of the screen aperture, a positively charged ion will be diverted into the direction of the closest edge of the accelerator aperture, and the particle leaves the thruster at a skewed angle. The magnitude of the skewed angle is roughly proportional to the offset between the two apertures, until ions impinge directly on the accelerator aperture electrode. For circular apertures, the direction of the diversion can occur anywhere in the radial plane. By manipulating the relative alignment between the screen and accelerator apertures, the entire beam from an ion thruster can be collectively steered in a desired direction. This could effectively provide a spacecraft with a means of thrust vector control.

A series of design studies took place in the early 1970s with the goal to develop thrust vectoring techniques for ion thrusters via grid manipulation. One significant design effort involved a complex array of accelerator electrodes that could be differentially charged to divert exiting ions.[1] The 5 cm diameter thruster had absolutely no moving parts, but it did contain dozens of electrode elements which needed to be isolated at high voltage. Experimental tests of the concept were fairly successful, however, insulator plating and excessive electrode erosion were viewed as serious life limiting issues.

Mechanical grid translation was also considered in early work. The phenomenon was originally regarded as an alignment concern when thermally induced distortion in the ion optics consequently buckled the grids, and diverted the exiting ion beam.[2] Careful analysis that followed resulted in a better understanding of asymmetric electrode effects, and confidence that this behavior might be exploited as a means of thrust vector control. Numerical simulations were performed, and it was concluded that beam deflection of 10 degrees should easily be obtained.[3] The approach was initially applied to 5 cm thruster optics designs, and produced encouraging results.[4] The screen grid was suspended in place by an arrangement of 8 helical springs connected tangentially around the grid perimeter. At uniform temperature, the opposed springs would cancel their tension and the screen and accelerator grids would be concentrically aligned. If electric current were sent through select springs, resistive heating and subsequent loss of tension would pull the screen grid out of alignment by an amount proportional to the temperature imbalance. The technique was mechanically simple, but movement was slow, and susceptible to interference from extraneous heat sources. Helical springs were also used with a 30 cm

screen grid, which was suspended radially instead of tangentially. This was a significantly larger grid size which, because it was flat, was much more susceptible to local thermally-induced buckling. There was serious discussion about using dished 30 cm grid optics, but no indication that this was actually tested with grid translation.

The theory of ion beamlet steering was more thoroughly developed in the later 1970s.[5] A theoretical relation between the plume deflection angle β, and the lateral grid translation ε was shown to be:

$$\beta = -14.3 \frac{\varepsilon}{\ell_g} \qquad (1)$$

measured in degrees, where ℓ_g represents the grid separation distance. Parametric tests were also performed, covering a wide range of aperture geometries.[6] Homa and Wilbur experimentally determined an empirical counterpart for equation 1 to be:

$$\beta = -15.8 \frac{\varepsilon}{\ell_g} \qquad (2)$$

Most grid translation work prior to 1980 had been carried out using mercury propellant operating in divergent field thrusters. Since 1980, xenon has emerged as a more favorable propellant due to its benign environmental impact, and simple gaseous propellant system. About the same time, divergent field magnetic designs were replaced by higher performing ring-cusp discharge chambers.[7] More recently, flight opportunities have moved hardware from the test chamber to actual space applications.[8] For example, the NSTAR thruster was used as primary propulsion on the interplanetary DS1 spacecraft. Boeing is using ion propulsion as a means of stationkeeping on it's commercial communications satellites. Ion propulsion is finally being considered as a practical and effective technology that can fulfill mission requirements. Thrust vector control is a logical area to expand system capability. The DS-1 spacecraft utilized a gimbal ring that was much more massive than the ion thruster being gimbaled. While that design choice helped reduce program risk, it also compromised mass savings made possible by the high performance propulsion. The DS-1 gimbal controlled

the thrust vector over a range of +/- 5 degrees in the roll and pitch directions.

One approach towards minimizing gimbal structural mass is to reduce the mass that the gimbal mechanism must support. Obviously, the grids of an ion thruster are much less massive than the thruster as a whole, but they are the sole component that determines the direction of the thrust vector. Hard mounting the discharge chamber offers an opportunity to simplify spacecraft interfaces, while increasing structural rigidity. The challenge for the designer is how to actively manipulate the ion optics while maintaining precise aperture geometry and control. Maximum translation between extreme positions is only on the order of a quarter mm total movement, but precise control must be maintained throughout this range while in a physically hostile environment. The translation mechanism must also survive launch vibration without damage or loss of alignment. This paper describes a simple and compact grid translation mechanism, and reports on laboratory performance measurements.

Description of Laboratory Thruster

The 30 cm ion thruster consisted of a mild steel discharge chamber, and modified 30 cm NSTAR ion optics.[9] An NSTAR-type neutralizer cathode assembly was installed on the ground screen, adjacent to the ion optics. Aside from three small motors located in the rear, the ion thruster looked ordinary, with a close-fitting cylindrical plasma screen.

The ion optics utilized the NSTAR design. Both grids were dished outward, and had a nominal beam diameter of 28 cm. The positive screen grid and negative accelerator grid were operated at voltage values indicated in Table 1. Two molybdenum grids, stiffening rings, and titanium mounting ring were essentially identical to those of NSTAR. The significant difference was that the rigid accelerator grid mounting posts were replaced with thin flexure rods. The rods were straight in the axial direction, maintaining a consistent gap between the screen and accelerator grids. They were flexible in the radial and azimuthal directions, allowing free movement parallel to the plane of the accelerator grid. A total of 12 flexures were evenly spaced at 30 degree intervals around the perimeter of the accelerator grid. It is important to note, however, that both grids were dished, which resulted in a 16 degree angle between

the grid plane and the actual edge of the grid. As a result, the grids moved relatively parallel near the centerline, but at a slight angle near the outer perimeter. The grid gap could thus change slightly near the edge of the grid during translation. Since the beam density is generally high at the center and low near the perimeter, it was believed that this non-ideal grid translation would not be a significant factor. This non-ideal movement was anticipated in earlier work of the 1970s, and was judged to be of no major significance.

Precise positioning of the accelerator grid relative to the screen grid was accomplished with three reed flexure assemblies linked to the accelerator grid. A diagram of one reed flexure assembly can be seen in Figure 1. Two individual flat flexures are joined by a 3 mm thick spacer. When the spacer is twisted, the free ends of the flexures are translated a distance proportional to the angle of twist. This results in very small, but very repeatable, relative movement of the flexure ends. Three of these assemblies were attached tangent to the accelerator grid at 120 degree intervals. They control movement only in the tangential direction, but allow free motion in the radial direction. By coordinating their operation, the reed flexures can collectively translate the accelerator grid in the X, Y, and azimuthal directions relative to the screen grid (see figure 2). Twisting of the flexure spacer is accomplished through an insulative ceramic shaft leading out the back of the thruster. Since all shaft control was by rotation, thermal expansion of various components had very little influence on grid translation. The shaft was free to move in the axial direction. Rotation of the shaft occurred through a sector gear and servo-motor. The servo-motors were commercially available, flying-model airplane devises, slightly modified to function with the analog control system. A position sensor on each servo-motor provided feedback which was displayed digitally on the control panel. An analog control system allowed the user to move each motor individually, or coordinate all three motors collectively to perform X and Y translation, and w rotation. Translation rates were fast, allowing full range of movement in about 1 second. The translation mechanism had a capacity to permit tangential movement of the accelerator grid of +/- 0.4 mm with respect to the neutral position of the screen.

The analog control system was configured to simplify user-specified grid position. Grid position was dialed

in, specifying desired X, Y, and w coordinates. The X direction was purely horizontal, the Y direction was vertical, and the w (azimuthal) direction was pure rotation of the accelerator grid relative to the screen. These inputs were then divided and modified to account for reed flexure locations and the geometric reference frame. Summation amplifiers establish a theoretical position for each of the three servo-motors, which was used as a reference signal to compare with the actual position. Three proportional control loops then drive each actual position in the direction of the theoretical position, thus executing the command.

Description of Test Facility

Tests were performed under vacuum in a 2.2 m diameter by 9 m long, horizontally oriented facility. Seven helium cryotubs provided pumping speed of approximately 10^5 liters per second, and maintained pressures on the order of 1 mPa during thruster operation. The thruster was geometrically aligned to exhaust down the center axis of the facility, thus minimizing the flux of back-sputtered material.

Electric power was provided to the thruster using rack-mounted laboratory power supplies. The rack was located in a control room approximately 15 m from the thruster. Thruster operating parameters were measured using isolated digital multimeters which were also in the control room.

Xenon propellant was supplied to the discharge cathode, neutralizer cathode, and main discharge chamber. All three flows were controlled and metered separately using commercially available flow controllers. The xenon storage bottle, pressure regulator, and flow controllers were located adjacent to the vacuum facility in the vicinity of the thruster. Flow rates were input from the control room, and corresponded to specifications in the NSTAR throttling table.[10]

A movable Faraday probe was used to collect plume data across the ion beam. A two-dimensional positioning track allowed near-field horizontal probe sweeps to be taken within millimeters of the accelerator grid, or far-field sweeps 1.2 m downstream of the exit plane. The probe location was computer-controlled through two stepping motors on the two dimensional track. Probe signal data was digitized, and stored in data files. Figure 3 shows

typical probe sweep data through the thruster plume. The probe signal gradually increased in magnitude until it reaches a maximum roughly half way through the plume. The signal then gradually decreased, revealing a Gaussian-like curve shape. The position of the maximum signal was assumed to correspond with the center of the beam, and could be tracked as the plume was diverted during grid translation.

Test Procedure

The first use of the experimental hardware involved displacement calibration exercises in order to correlate input commands with accelerator grid movements. This was done separately for X, Y, and w inputs. Once the mechanical response was thoroughly characterized, the test thruster was installed in the vacuum facility.

Initial thruster operation was conducted with the accelerator grid in the center location so that conventional performance could be verified. At that point, input commands for X, Y, and w were systematically varied, while thruster response was monitored. Electron backstreaming, ion optics perveance, and beam current density profile data were obtained at various power levels and translation positions. The thruster operating parameters were recorded manually, while plume probe measurements were recorded with a digital data acquisition system. Direct thrust measurements were not taken. The thruster was primarily operated at three power levels throughout all testing. These were based on NSTAR power levels TH4, TH10, and TH15, corresponding to 0.98 kW, 1.7 kW, and 2.3 kW, respectively. Table 1 lists typical thruster operating parameters used and discussed throughout this work.

The *impingement-limited total voltage* was determined by incrementally reducing beam power supply voltage at a fixed beam current and observing when accelerator current increased rapidly. The point where accelerator current increased by more than 0.2 mA per 10 volt reduction in beam voltage was identified as the *impingement-limited total voltage*. The effective reduction in total voltage to reach this point was identified as perveance margin. The electron backstreaming limit was determined by incrementally reducing accelerator voltage at a fixed beam power supply voltage until beam current increased by 0.1 mA. The accelerator voltage at that

point was identified as the electron backstreaming limit.

Results

Calibration of Input Commands

The grid translation mechanism underwent a series of bench-top calibration exercises in order to characterize its mechanical response to input commands. A machinist's dial gage was applied to the perimeter of the accelerator grid to quantify displacement in the radial plane. The dial gage was designed to measure displacements over the range of 0 to 0.030 inches using 30 graduation marks, and it was practical to resolve down to 0.0002 inches with reasonable confidence. The inch units were then converted to SI units for subsequent analysis. Conversely, the control input setting was determined by a ten-turn potentiometer, and was readable at regular intervals from 000 to 999.

In the first exercise, the response of each reed flexure assembly was measured as a function of control input setting. The control setting was slowly increased, and recorded when the dial gage passed certain graduation increments. The result was a look-up table for each reed flexure which indicated the input setting necessary to obtain a desired accelerator grid displacement. The response of all three reed flexure assemblies were analyzed for output sensitivity, linearity, and cross-axis interaction. While non-ideal behavior was identified, it was concluded that the position of each reed flexure assembly was known to within 0.025 mm.

A second exercise was performed to characterize the integrated response of the analog control system. Instead of separate input commands for each reed flexure assembly, responses were coordinated so that X, Y, and w input settings controlled horizontal, vertical, and azimuthal movement, respectively. The dial gage was positioned to measure radial and tangential movement at top, bottom, and side locations on the accelerator grid. Again, it was concluded that the position of the grid was known to within 0.025 mm. A look-up table was generated using these results, and would later be used to control the grid position during actual thruster operation.

The high voltage breakdown strength of the grid translation thruster was checked, and showed no unusual current leakage.

The thruster was installed within a 2.3 m diameter vacuum facility as described previously. Hollow cathode conditioning took place, followed by operation of the discharge chamber under low voltage. This action preheated the entire thruster assembly, baking out volatiles, and providing an opportunity to observe the response of the servo-motor position sensors. The motors were located in back of the thruster ground screen, and showed little temperature rise or position drift.

Nominal Operation under Vacuum

Initial thruster tests took place with the accelerator grid in the *nominal design position*- this being the best coaxial alignment possible with the aid of a 20X microscope. The objective was to characterize the operation of the grid translation thruster, and verify that it behaved in a manor consistent with conventional 30 cm thrusters. Only 10 amps of discharge current was needed to obtain maximum beam output (TH15), compared to the typical 13 A for NSTAR. This probably resulted from the more effective mild steel chamber wall used here, which performed better than the non-magnetic NSTAR wall. Accelerator current was 5.6 mA, which was slightly better than typical for TH15. It was concluded that this thruster performed slightly more efficiently than an average 30 cm design, but not abnormally so.

Effects of Grid Translation

Tests continued in which the accelerator grid was translated in the X direction. A quick mapping was performed, where accelerator grid impingement current was plotted against grid position. The objective was to find an effective mid-point along the X-axis such that impingement current would be symmetric for grid movement in either direction. It would also indicate the maximum practical displacement range before impingement current became prohibitive. As can be seen in Figure 4, impingement current increased from a base level of 6 mA to about 16 mA when the grid is translated 0.23 mm in either X direction. Similar results were also obtained in the Y direction where the impingement current increased to 14 mA as a result of 0.20 mm translation.

Effects of Grid Rotation

Less dramatic results were observed when the grid was rotated about the w axis. Impingement current increased from 6 to 8 mA when the perimeter was circumferencially translated 0.30 mm, corresponding to a rotation angle of 0.1 degrees. This was the largest angle the mechanism was capable of driving the accelerator grid past the center position. The comparatively small change in impingement current was not unexpected, considering that beam density is typically highest at grid center, and drops off significantly at larger radii. Grid rotation affects apertures near the perimeter more than the center, but beamlets near the perimeter are likely to be small, and thus result in less impingement. Results from the maps indicate that the grids were initially aligned fairly accurately, but this exercise identified a more precise center position.

Faraday probe sweeps were the most practical means to quantify the effect of grid translation on the exhaust plume. As stated previously, there was a characteristic signal peak in all probe sweeps that was attributed to maximum beam density at grid center. This signal peak would change its position along the X axis whenever the accelerator grid also moved along the X axis. Figure 3 shows three Faraday probe sweeps taken at TH4, all at identical operating conditions except that the accelerator grid was in a different position during each sweep. The center trace shows the beam profile with the grid in the normal center position. The left and right trace shows beam profile with the accelerator grid translated +0.25 mm and -0.25 mm, respectively. In those two cases, the density peak was shifted 122 mm to the left, and 125 mm to the right, respectively. The beam deflection angle was simply calculated by triangulating the downstream distance with the peak shift distance. Beam deflection angles were measured at TH15 for grid translations ranging -0.20 mm through +0.20 mm, and plotted in Figure 5a. A grid translation of 0.20 mm resulted in a plume angle of -7 degrees. Grid translation beyond 0.02 mm resulted in excessive acceleration current, as shown in the figure. A linear curve fit of *plume deflection angles* at power level TH15 (2.3 kW) show a slope of

$$\frac{\beta}{\varepsilon} = \frac{-13.8 \deg}{0.4 mm} \qquad (3)$$

By rearranging terms, and substituting in grid gap to non-dimensional grid translation units, the above relation can be transformed into:

$$\beta = -22.8 \frac{\varepsilon}{\ell_g} \qquad (4)$$

Similar results were obtained at power level TH4 of 0.98 kW, and power level TH10 of 1.3 kW. Plume deflection measurements for these are shown in Figures 5b, and 5c, yielding the empirical correlations:

$$\beta = -16.5 \frac{\varepsilon}{\ell_g} \qquad (5)$$

at TH4, and

$$\beta = -21.4 \frac{\varepsilon}{\ell_g} \qquad (6)$$

at TH10. Results from TH4 came to within 4% of data obtained by Homa and Wilbur (see equation 2). The variation in plume deflection slopes at the three power levels was unexpected, and somewhat puzzling. The coefficient obtained at TH10 was 50% higher than theoretical, and the coefficient obtained at TH15 was almost 60% higher. One possible explanation is that the higher beam current at higher power levels affected the plasma sheath inside the aperture region. This, however, is contrary to the results of Homa and Wilbur, who found this to be a weak effect. A more likely explanation is that the gap between the screen and accelerator grids became smaller at higher power levels. With convex dished grids, the higher temperature screen grid tends to expand, and bow outward towards the cooler accelerator grid. This distortion of grid gap becomes worse at higher power levels, and has even been known to cause grid-to-grid contact.[11] As shown in equation (5), when grid gap ℓ_g is reduced, the plume deflection angle β increases. If this explanation is correct, then the decimal coefficients in equations (4) - (5) may actually be the same number, but with a variable grid gap. Assuming the lowest power level of TH4 provides the most accurate coefficient, it should be possible to estimate the grid gap which was present during tests at TH10 and TH15. If equation (4) is correct for a grid gap of 0.66 mm at TH4, then the grid gap at TH10 would be 0.51 mm, and the grid gap at TH15 would be 0.48 mm.

A more complete understanding and verification of grid gap variation is clearly necessary before a grid

translation mechanism is implemented on a flight thruster. Accurate characterization of thrust vector response will be needed in order to write control law software. The complexity of this task could be reduced, however, through the use of zero expansion materials, such as carbon-carbon composites.

Other Observations

One topic that can be investigated with the grid translation mechanism is the impact of grid alignment on thruster performance. There is interest in knowing how accurate ion optics must be aligned in order for them to meet performance requirements. Conversely, how much can performance improve simply by aligning the screen and accelerator grids more precisely? An attempt was made to answer this question by measuring perveance margin and electron backstreaming as a function of accelerator grid position. Radial displacements were imposed on the ion optics at specific intervals, and results are shown on Figure 6a. At throttle point TH15, perveance margin varied from a high of 390 volts, to a low of 30 volts when translated 0.20 mm. The electron backstreaming limit varied from a maximum of –125 volts to a minimum of -112 volts when translated 0.20 mm. While it may be increasingly more difficult for xenon ions to exit the grids at high translation, it is also more difficult for electrons to backstream in. Notice that in both measurements, the variation was fairly smooth, and tended to level out asymptotically near center alignment. Slightly better performance resulted at TH4, where beamlet size and space charge effects are reduced (see figure 6b). Perveance margin was reduced from 450 volts to 100 volts when translated 0.25 mm. Performance at TH10 fell between that of the high and low power levels (see figure 6c). A similar effect on perveance and electron backstreaming were seen by rotating the accelerator grid in the w direction. Figure 7a shows that perveance margin was reduced to about 60 volts by rotating the grid 0.1 degrees. At lower power levels, the perveance was not impacted as severely by grid rotation. (see Figures 7b and 7c)

Conclusions

Data were obtained from a 30 cm xenon ion thruster in which the accelerator grid was translated in the radial plane. The thruster was operated at three different throttle power levels, and the accelerator grid was incrementally translated in the X, Y, and azimuthal directions. Plume data was obtained

downstream from the thruster using a Faraday probe mounted to a positioning system. Successive probe sweeps revealed variations in the plume position. Thruster perveance, electron back-streaming limit, accelerator current, and plume deflection angle were determined at each power level, and for each accelerator grid position. Results showed that the thruster plume could easily be deflected up to 6 degrees without a prohibitive increase in accelerator impingement current. Results were similar in both X and Y directions. An azimuthal rotation could be applied to the thruster plume, which was observed by watching plume divergence increase.

Plume data presented above show that this thruster was effective at diverting the path of the ion beam. The plume direction was easily controllable along two axis, but it must be verified that there are no adverse consequences on thruster life. Many issues must be addressed before such a technique is employed on practical spacecraft. Grid erosion and its potential impact on thruster life is an obvious concern that must be investigated. Periods of increased erosion may be considered acceptable as long as they are limited in duration, and pose a small fraction of overall mission use. Unfortunately, grid erosion measurements goes beyond the scope of this work.

References

[1] Lathem, W.C., "1000-Hour Test of a Dual Grid Elecrostatic Bean Deflection Accelerator System on a 5-Centimeter-Diameter Kaufman Thruster, "NASA TM X-67907, August 1971.

[2] Lathem, W.C., "Approximate Analysis of the Effects of Electrode Misalignment on Thrust Vector Control in Kaufman Thrusters," NASA TM X-52369, January 1968.

[3] Lathem, W.C., and Wallace, Adam B., "Theoretical Analysis of a Grid-Translation Beam Deflection System for a 30-cm Diameter Kaufman Thruster, "NASA TM X-67911, August, 1971.

[4] Lathem, W.C., "Grid-Translation Beam Deflection System for 5-cm and 30-cm Diameter Kaufman Thrusters," NASA TM X-68029, April 1972.

[5] Whealton, J.H., "Linear Optics Theory for Ion Beamlet Steering,"*Rev. of Sci. Instru.*, Vol. 48, pp. 1428-1429, 1977.

[6] Homa, J.M., and Wilbur, P.J., "Ion Beamlet Vectoring by Grid Translation," AIAA Paper 82-1895, November 1982.

[7] Sovey, J.S.,"Improved Ion Containment Using a Ring-Cusp Ion Thruster," *Journal of Spacecraft and Rockets*, Vol. 21, No. 5, 1984, pp 488-495.

[8] Sovey, J.S. and Rawlin, V.K, "A Synopsis of Ion Propulsion Development in the Unites States: SERT 1 to Deep Space 1,"AIAA Paper 99-2270, June 1999.

[9] Sovey, J.S., et. al., "Development of an Ion Thruster and Power Processor for New Millennium's Deep Space 1 Mission," AIAA Paper 97-2778, July 1997.

[10] Rawlin, V.K., et al., "NSTAR Flight Thruster Qualification Testing," AIAA Paper No. 98-3936, July 1998.

[11] Soulas, G.C., et al., "Performance of Titanium Optics on a NASA 30 cm Ion Thruster," AIAA paper No. 2000-3814, July 2000.

Table 1.—Thruster operating points

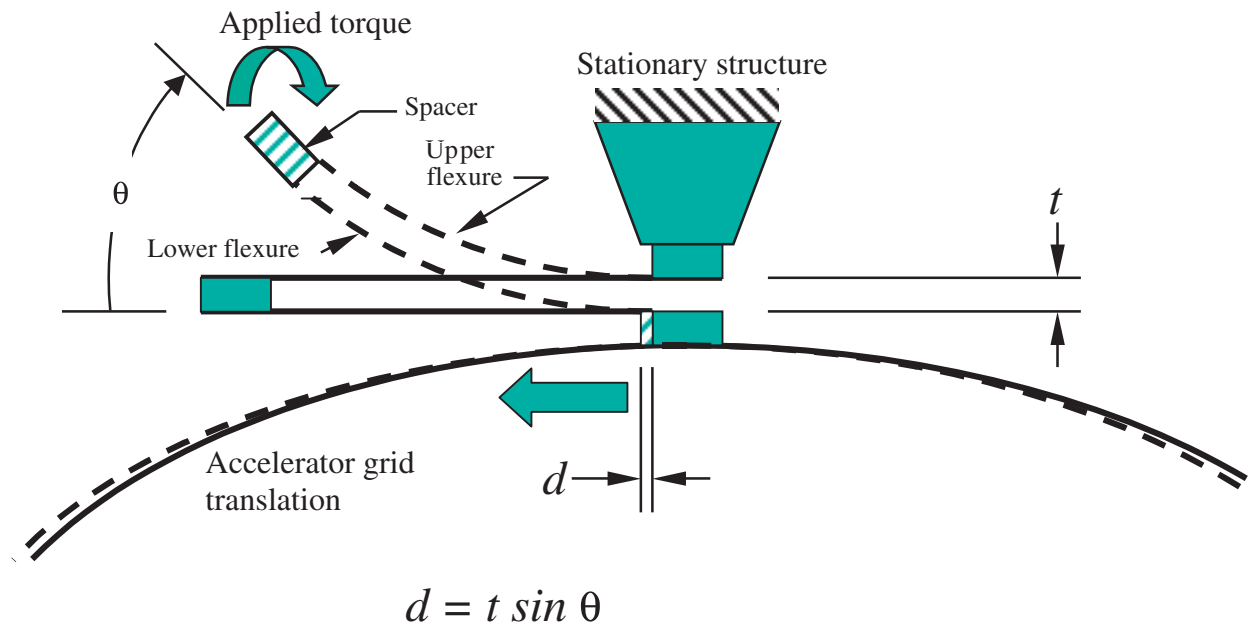| Power Level	Beam Current, A	Beam Voltage	Accel. Voltage	Input Power, kW
TH4	0.71	1100	−150	0.98
TH10	1.3	1100	−180	1.7
TH15	1.76	1100	−180	2.3

$$d = t \sin \theta$$

Figure 1.—Diagram of differential reed flexure assembly
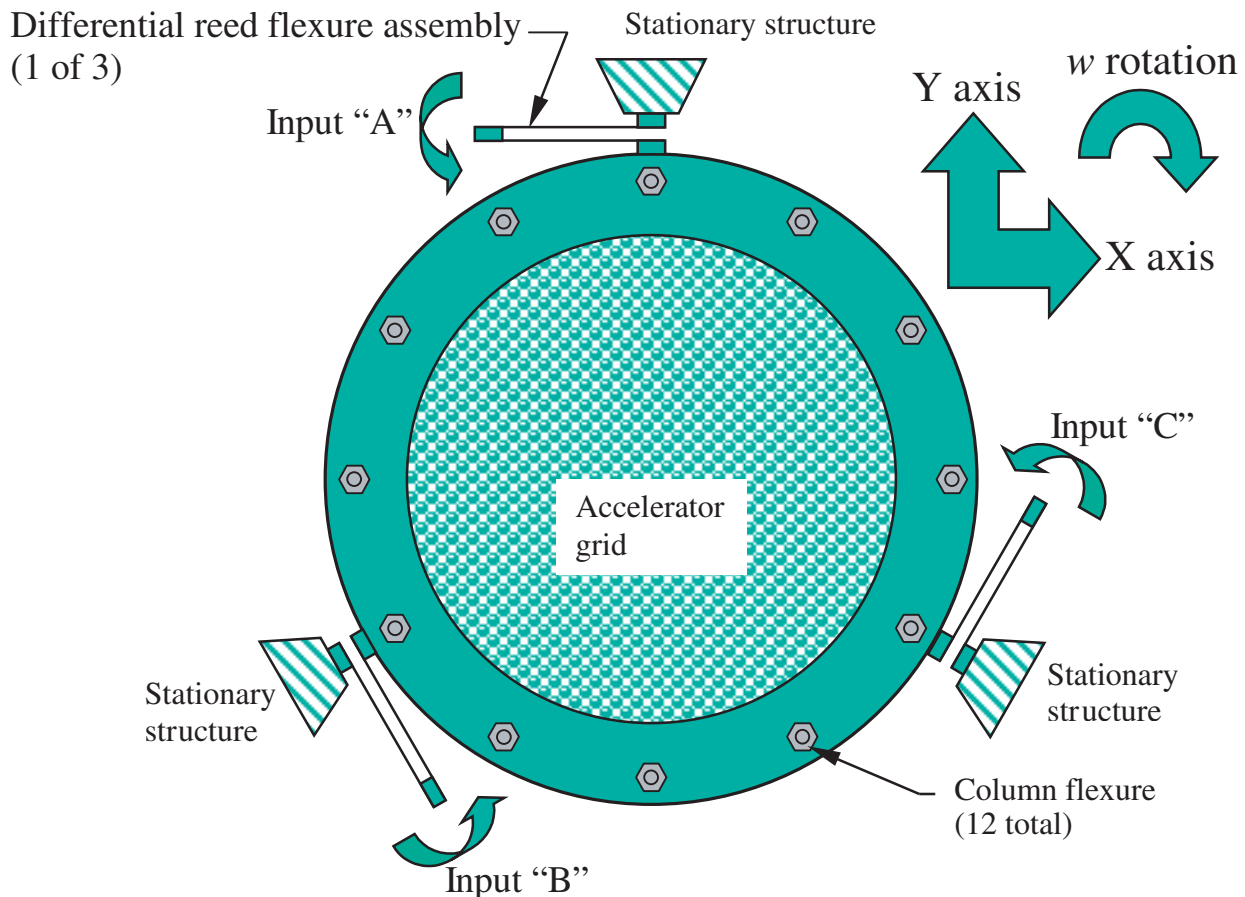
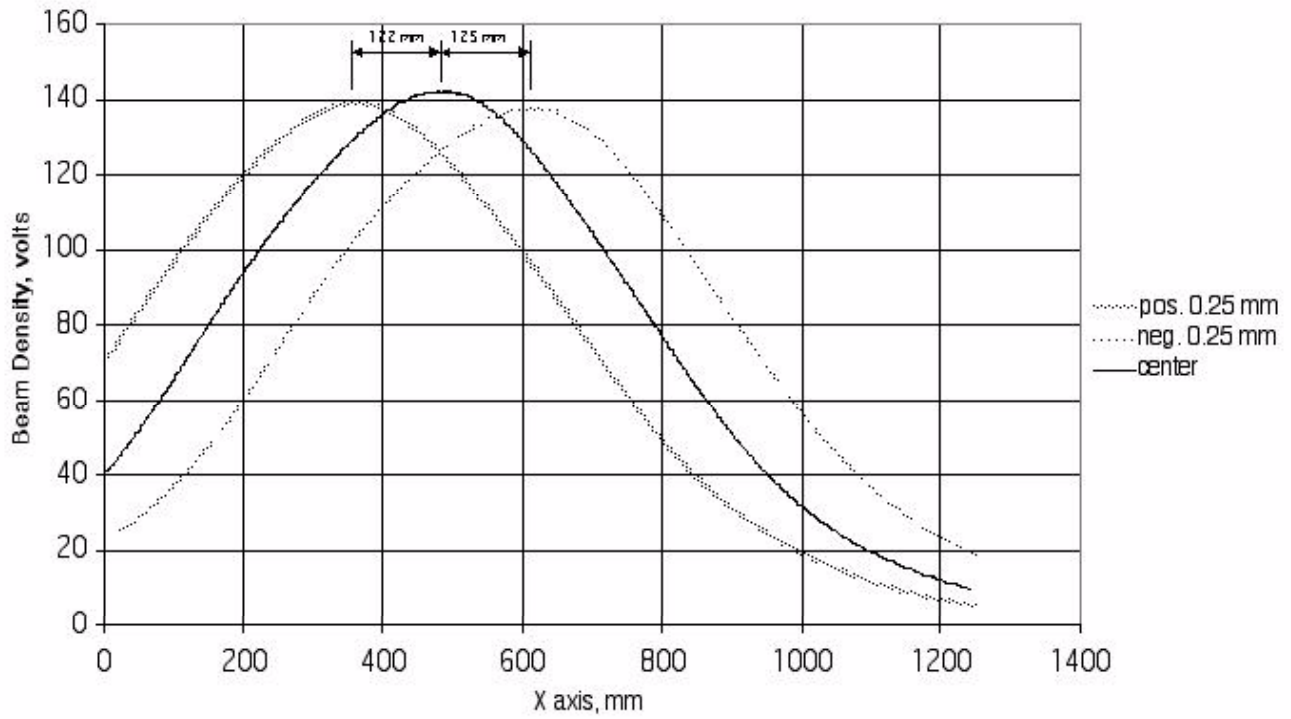Figure 2.—Diagram of grid translation mechanism and reference frame.

Figure 3.—Faraday probe sweep across beam taken 1.175 meters downstream.

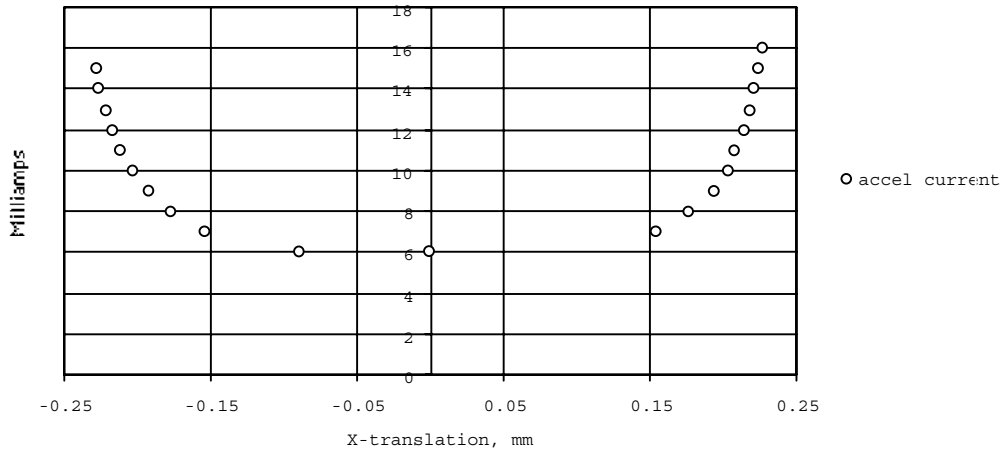Figure 4a.—Accel Grid Impingement, TH15 vs X-translation.

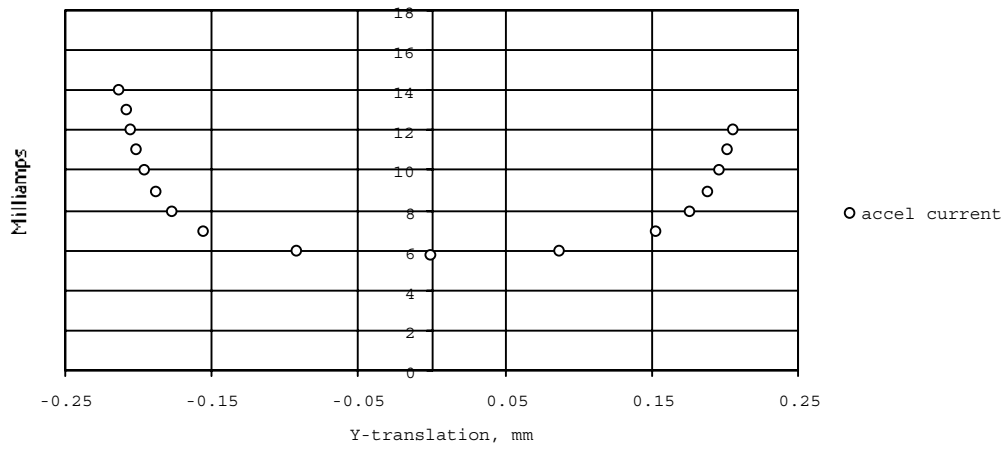Figure 4b.—Accel Grid Impingement, TH15 vs Y translation.

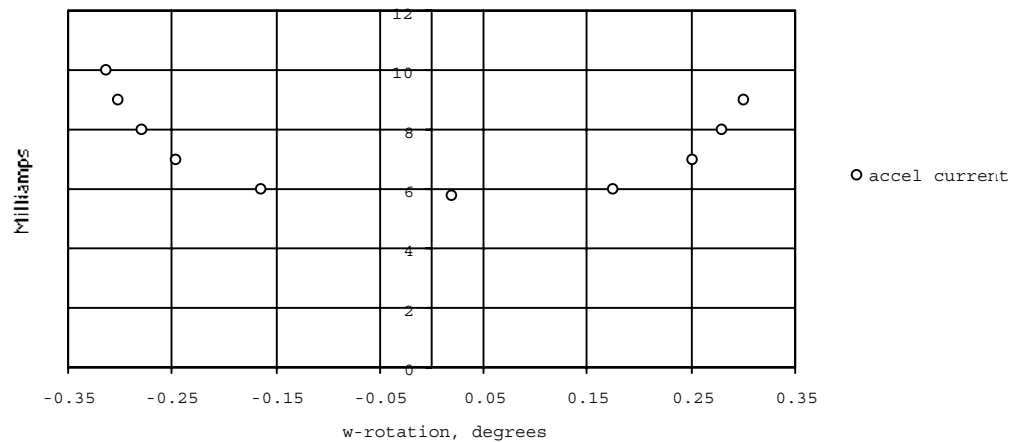Figure 4c.—Accel Grid Impingement, TH15 vs W (rotation).
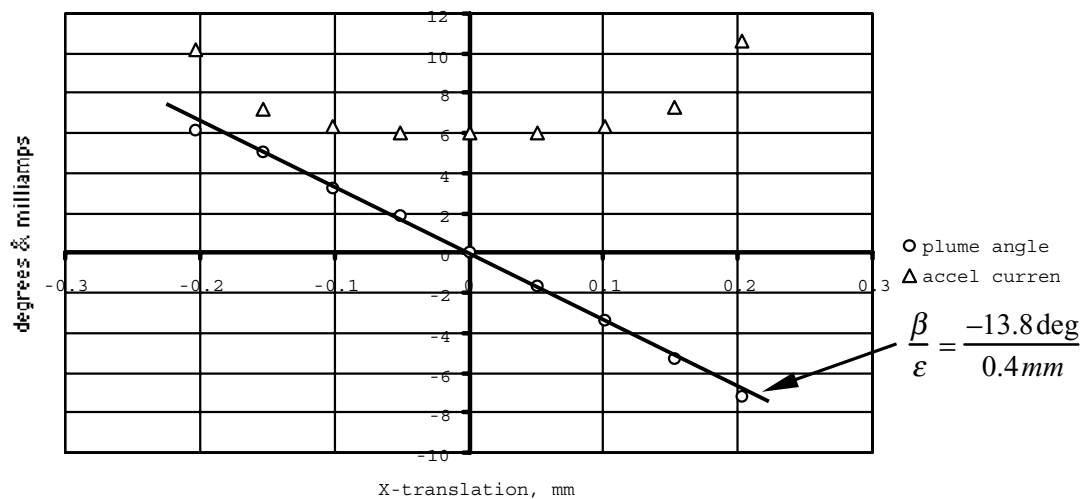

10

Figure 5a.—X Translation, TH15.

$$\frac{\beta}{\varepsilon} = \frac{-13.8\,\text{deg}}{0.4\,mm}$$

X-translation, mm

Figure 5b.—X Translation, TH4.

$$\frac{\beta}{\varepsilon} = \frac{-10.0\,\text{deg}}{0.4\,mm}$$
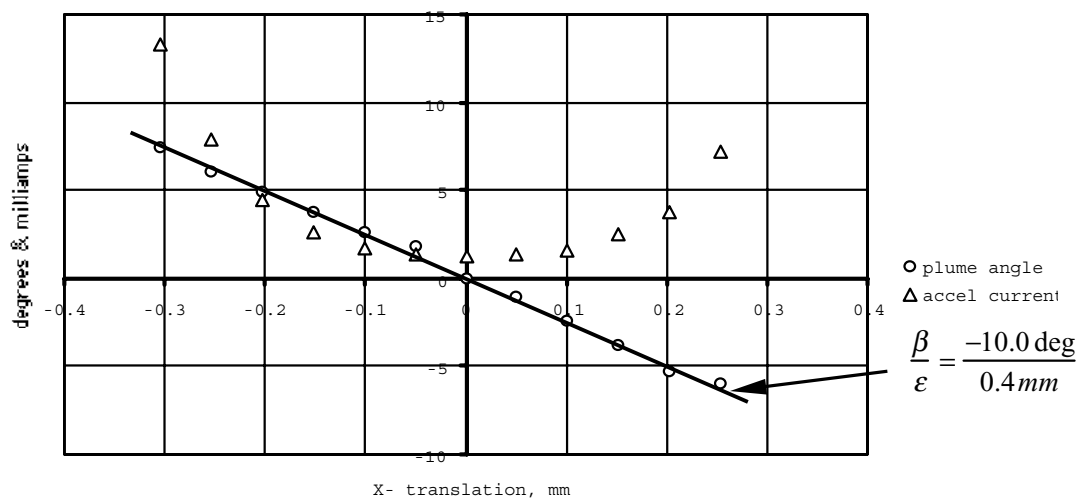
X- translation, mm

Figure 5c.—X Translation, TH10.

$$\frac{\beta}{\varepsilon} = \frac{-12.9\,\text{deg}}{0.4\,mm}$$
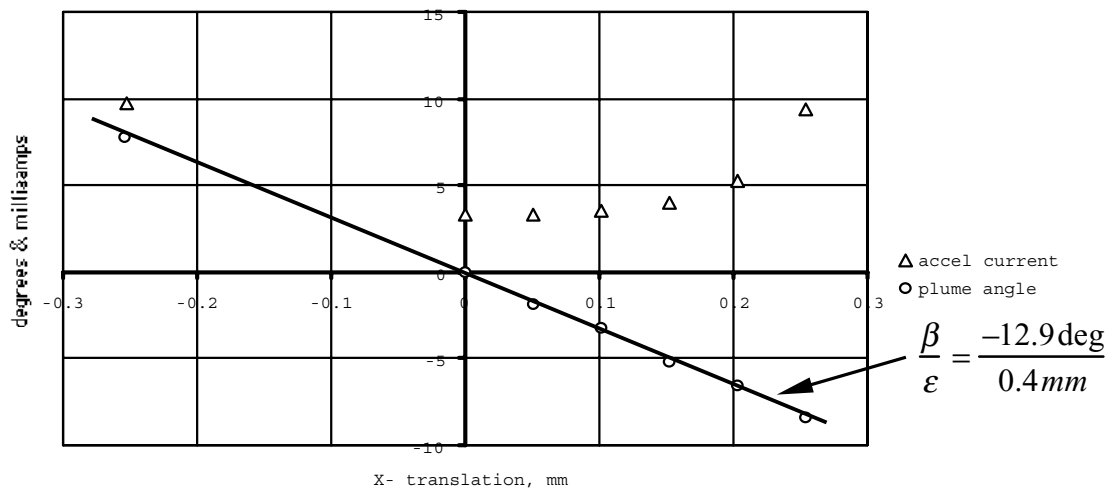
X- translation, mm

Figure 6a.—X Translation, TH15.
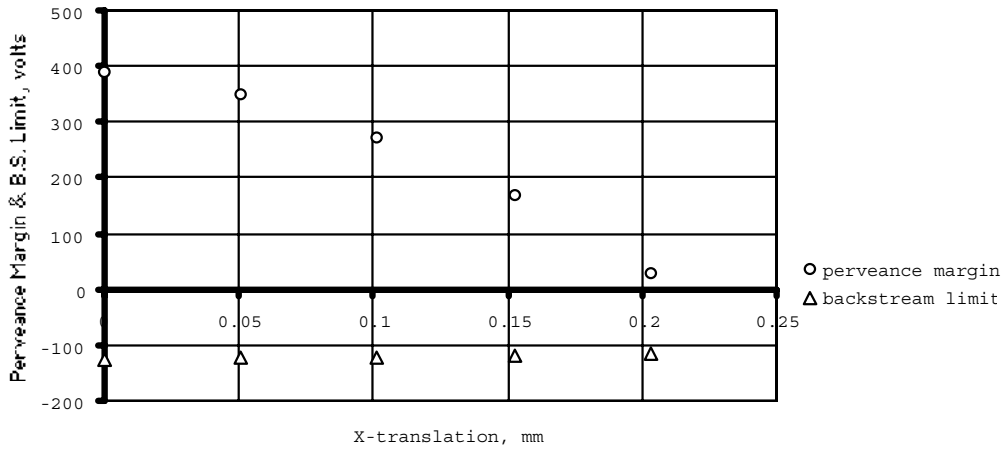
X-translation, mm

Figure 6b.—X Translation, TH4.
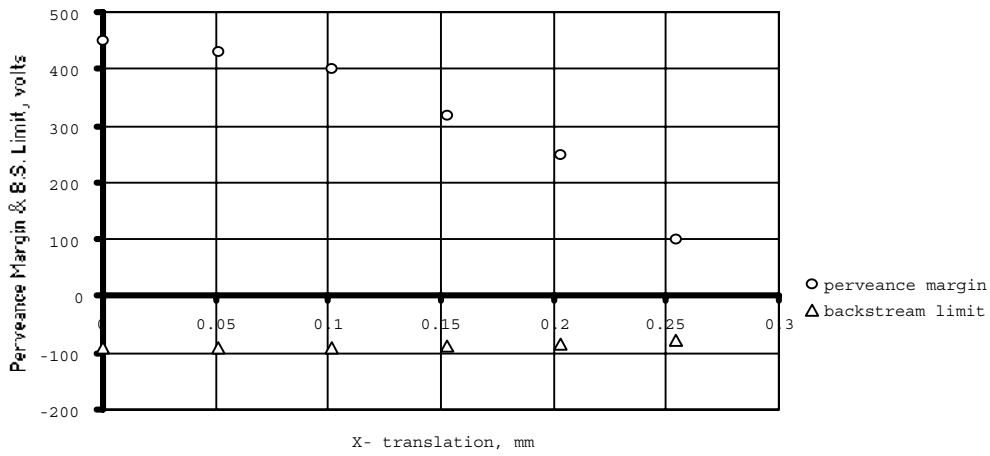

X- translation, mm
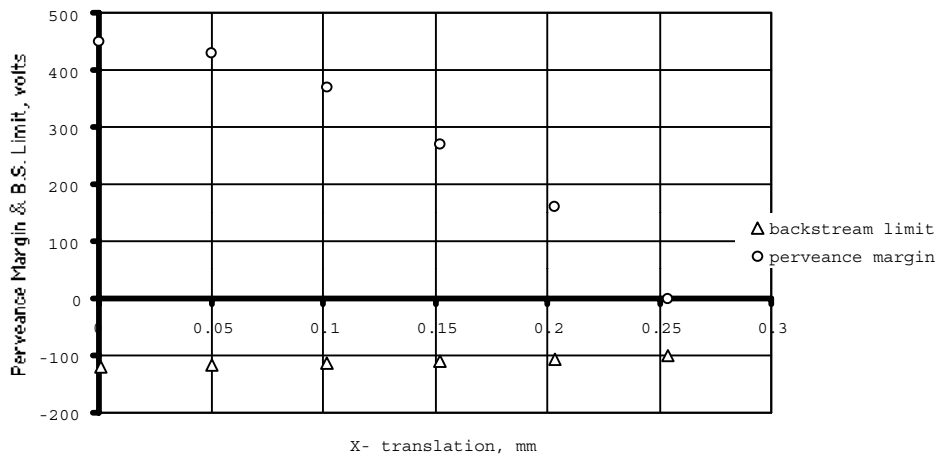
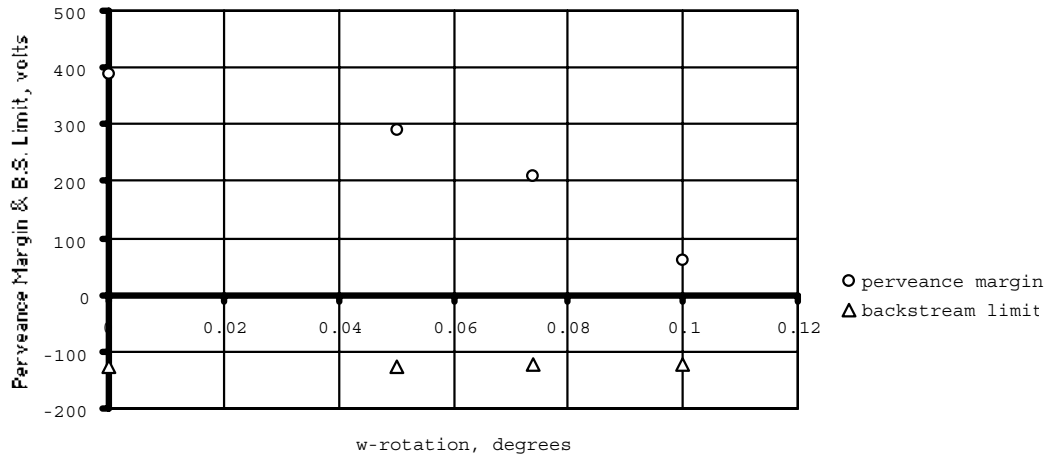Figure 6c.—X Translation, TH10.

X- translation, mm

Figure 7a.—w Rotation, TH15.

Figure 7b.—w Rotation, TH4.
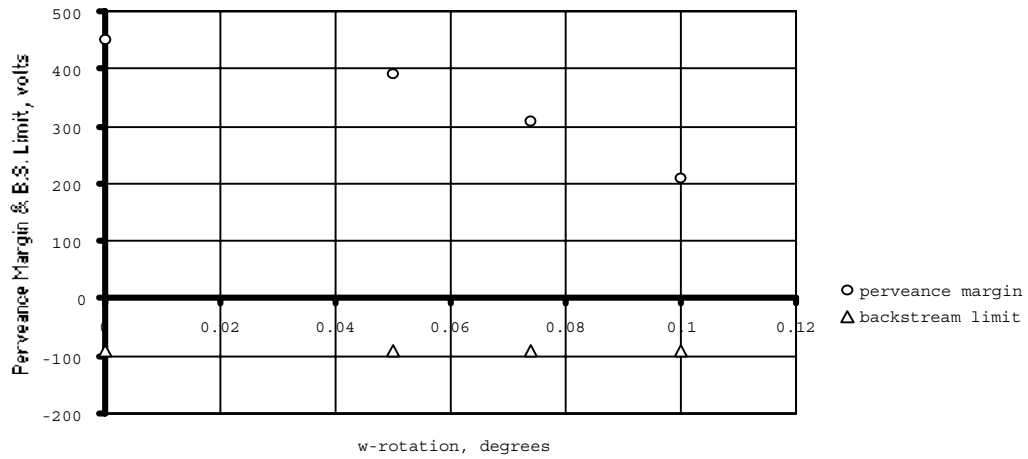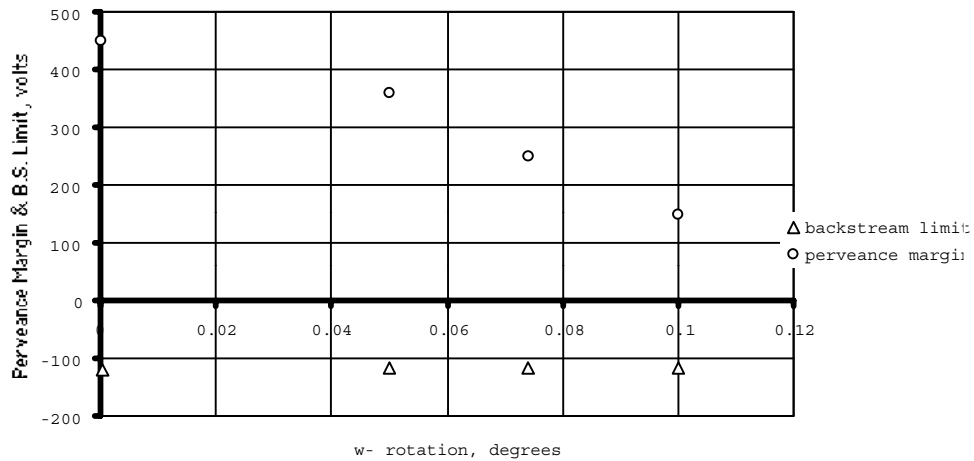

Figure 7c.—w Rotation, TH10.

REPORT DOCUMENTATION PAGE

Public reporting burden for this collection of information is estimated to average 1 hour per response, including the time for reviewing instructions, searching existing data sources, gathering and maintaining the data needed, and completing and reviewing the collection of information. Send comments regarding this burden estimate or any other aspect of this collection of information, including suggestions for reducing this burden, to Washington Headquarters Services, Directorate for Information Operations and Reports, 1215 Jefferson Davis Highway, Suite 1204, Arlington, VA 22202-4302, and to the Office of Management and Budget, Paperwork Reduction Project (0704-0188), Washington, DC 20503.

1. AGENCY USE ONLY (*Leave blank*)	2. REPORT DATE June 2002	3. REPORT TYPE AND DATES COVERED Technical Memorandum

4. TITLE AND SUBTITLE

Translation Optics for 30 cm Ion Engine Thrust Vector Control

5. FUNDING NUMBERS

WU–755–B4–04–00

6. AUTHOR(S)

Thomas Haag

7. PERFORMING ORGANIZATION NAME(S) AND ADDRESS(ES)

National Aeronautics and Space Administration
John H. Glenn Research Center at Lewis Field
Cleveland, Ohio 44135–3191

8. PERFORMING ORGANIZATION REPORT NUMBER

E–13268

9. SPONSORING/MONITORING AGENCY NAME(S) AND ADDRESS(ES)

National Aeronautics and Space Administration
Washington, DC 20546–0001

10. SPONSORING/MONITORING AGENCY REPORT NUMBER

NASA TM—2002-211502
IEPC–01–116

11. SUPPLEMENTARY NOTES

Prepared for the 27th International Electric Propulsion Conference cosponsored by the AFRL, CNES, ERPS, GRC, JPL, MSFC, and NASA, Pasadena, California, October 14–19, 2001. Responsible person, Thomas Haag, organization code 5430, 216–977–7423.

12a. DISTRIBUTION/AVAILABILITY STATEMENT	12b. DISTRIBUTION CODE
Unclassified - Unlimited Subject Category: 20 Distribution: Nonstandard Available electronically at http://gltrs.grc.nasa.gov/GLTRS This publication is available from the NASA Center for AeroSpace Information, 301–621–0390.	

13. ABSTRACT *(Maximum 200 words)*

Data were obtained from a 30 cm xenon ion thruster in which the accelerator grid was translated in the radial plane. The thruster was operated at three different throttle power levels, and the accelerator grid was incrementally translated in the X, Y, and azimuthal directions. Plume data was obtained downstream from the thruster using a Faraday probe mounted to a positioning system. Successive probe sweeps revealed variations in the plume direction. Thruster perveance, electron backstreaming limit, accelerator current, and plume deflection angle were taken at each power level, and for each accelerator grid position. Results showed that the thruster plume could easily be deflected up to 6 degrees without a prohibitive increase in accelerator impingement current. Results were similar in both X and Y direction.

14. SUBJECT TERMS	15. NUMBER OF PAGES 19
Electric propulsion; Ion thruster	16. PRICE CODE

17. SECURITY CLASSIFICATION OF REPORT	18. SECURITY CLASSIFICATION OF THIS PAGE	19. SECURITY CLASSIFICATION OF ABSTRACT	20. LIMITATION OF ABSTRACT
Unclassified	Unclassified	Unclassified	

NSN 7540-01-280-5500

Standard Form 298 (Rev. 2-89)
Prescribed by ANSI Std. Z39-18
298-102